Int. J. Solids Structures Vol. 23, No. 5, pp. 569–579, 1987
Printed in Great Britain.

0020-7683/87 $3.00+.00

THE ANALYSIS OF MULTIAXIAL CYCLIC PROBLEMS WITH AN ANISOTROPIC HARDENING MODEL

CHIN-CHAN CHU
Ford Motor Company, Dearborn, MI 48121, U.S.A.

(*Received* 4 *December* 1985; *in revised form* 17 *April* 1986)

Abstract—A recently-developed constitutive model that accounts for anisotropic hardening in a very general manner is applied to four strain-controlled multiaxial cyclic problems. The constitutive model is a generalization of the Mróz multiple yield surface concept to a continuous field of yield surfaces, and results of the four problems analyzed demonstrate that the model predicts stress–strain relationships remarkably close in qualitative behavior to experimental measurements. Concerns voiced previously that the Mróz model requires excessive memory capacity in numerical analysis are shown to be rendered invalid, except for cases containing loading cycles of diminishing amplitude. Further discussion addresses the fact that this constitutive model in its present simplest form, being cyclically stable, will require modifications when the effects of cyclic hardening/softening and cyclic creep/relaxation on the material behavior become significant.

INTRODUCTION

For materials subjected to monotonic loading, the classical flow theory of plasticity has been well accepted to give adequately accurate predictions of stress and strain states. However, a large number of structural components, e.g. in the automotive and aerospace industries, experience multiaxial cyclic loading conditions. Since the isotropic hardening rule employed in classical flow theory cannot predict the material behavior in many of the cyclic experiments, much effort in recent years has been focused on the establishment of a model which can properly account for the influence of complex loading histories on subsequent deformation.

Among the proposed models, the most widely discussed appear to be: kinematic hardening rules[1, 2] and two-surface theories (see, e.g. Ref. [3]), both types being based on the yield surface concept, and endochronic theories (see, e.g. Ref. [4]), which are based on the internal variable concept. Although all of these theories can be written in general three-dimensional forms, they are usually employed in uniaxial cyclic problems, and very few multiaxial cyclic applications can be found in the literature. This lack of extensive experimental verification of the models is mainly attributable to the substantial amount of computation necessitated by these theories in simulating complex loading conditions, and to the limited number of existing test data with which the analytical results can be compared.

From a theoretical point of view, the above-mentioned models also have the disadvantage of containing degrees of arbitrariness in the formulation. Specifically, there are various ways to define flow stress for kinematic hardening models since the yield surface size, which is conventionally related to flow stress, is assumed constant in the theory. For two-surface theories, the hardening rate of the material at an intermediate stress state between the yield and the loading surface, as well as the progression of the loading surface, are not uniquely defined. Finally, in order to simulate increasingly complicated phenomena the number of material constants in endochronic theories appears to increase unrestrictedly.

A recently developed constitutive model[5], although not yet sophisticated enough to include all observed features of cyclic behavior, appears to contain no such arbitrariness. This model is a generalization of Mróz's discrete multiple yield surface concept[6]. A continuous field of yield surfaces is assumed, but subsequently the same line of development as the classical flow theory is followed, producing a similarly compact incremental stress–strain relationship.

In this paper, the applicability of this generalized model is demonstrated by comparing the predicted results with experimental data on four cyclic tension–torsion problems. The good qualitative agreement obtained encourages further exploration in this direction to develop a simple constitutive equation of general validity.

THE CONSTITUTIVE MODEL

The model proposed in Ref. [5] assumes the existence of a field of continuously distributed yield surfaces in deviatoric stress space. These surfaces are concentric about the zero stress state for materials free of residual stresses. The size of the yield surface specifies the flow stress level as well as the associated modulus.† The smallest yield surface therefore corresponds to initial yielding and provides an elastic modulus. The relative positions of the yield surfaces change only during *plastic deformation*, according to two rules: (1) the yield surfaces do not cross one another; (2) any yield surface with which the loading point is in contact moves (rigidly) with the stress state. As a result, in a plastic state, there are generally numerous mutually tangential yield surfaces at the loading point. When loading continues, all these yield surfaces translate forward with the stress state and the largest surface is defined as the *active* yield surface which determines the instantaneous modulus. If unloading should take place, the smallest yield surface, which will be encountered first by the unloading path, becomes the active surface.

If a von Mises type yield function is adopted, we have

$$f = 3/2 \cdot (\mathbf{s} - \boldsymbol{\alpha}):(\mathbf{s} - \boldsymbol{\alpha}) - k^2 = 3/2(\mathbf{r}:\mathbf{r}) - k^2 = 0. \tag{1}$$

Here $\mathbf{s}$ is the deviatoric part of stress tensor $\boldsymbol{\sigma}$, $\boldsymbol{\alpha}$ denotes the position tensor of the center of the yield surface and k is the equivalent flow stress. The yield surfaces are then spheres in deviatoric stress space with radii $\sqrt{(2/3)}k$.

With the rules described above, the distribution of the yield surfaces at any moment in the loading history is completely determined by any previous deformation experienced by the material. The current distribution then specifies how the yield surfaces will subsequently evolve for a given continuation of the deformation history.

An example is used to illustrate the rules. Figure 1 shows the yield surface distribution resulting from an essentially two-dimensional deformation which ends at stress state 3. Note that the continuously distributed yield surfaces between surfaces (1) and (2), which are all mutually tangential at stress point 1, are omitted since their positions are completely defined by those of (1) and (2). Similarly omitted are the yield surfaces between (2) and (3). This implies that an infinite number of loading paths can result in the same final stress state and leave the material with the same memory of histories. This memory then determines the material hardening rate during subsequent deformations. Two examples of these paths are illustrated in Fig. 1: the simplest piecewise proportional loading 0–1–2–3, and a much more complex one with continuous mode variations and additional small loops. The two paths differ from each other merely by the amount of total strain accumulated and plastic work done. At the current stress state 3, depending on whether unloading or continued loading occurs, it is either the dotted subsequent yield surface or the solid loading surface (3), respectively, that determines the instantaneous modulus. The corresponding directions in which the yield surfaces will move upon further *plastic* deformation, are denoted, respectively, by the unit tensors $\boldsymbol{\beta}^u$ and $\boldsymbol{\beta}$ in the figure. The yield surface center, accordingly, moves by the amount of $\sqrt{(2/3)}\,\mathrm{d}k$ for every flow stress increment $\mathrm{d}k$; that is

$$\mathrm{d}\boldsymbol{\alpha} = \sqrt{(2/3)}\,\mathrm{d}k \cdot \boldsymbol{\beta}. \tag{2}$$

† The continuous yield-surface generalization was also reached earlier by Mróz and co-workers[7–9]. The formulations in Refs [7–9], however, adopted a different rule for the determination of tangent modulus during plastic deformation. They thus do not use the universal stress–strain curve concept as in classical plasticity theory, and is essentially equivalent to a two-surface theory.

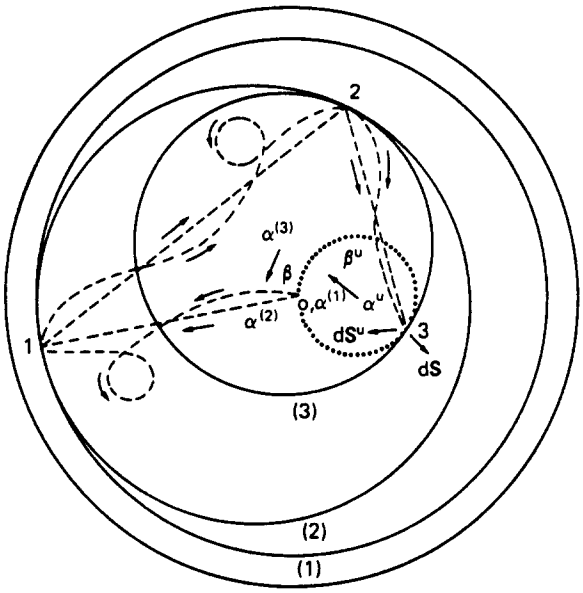

Fig. 1. A sketch of the yield surface distribution in deviatoric stress space after elastic–plastic deformation.

From the consistency condition, which states that the plastic loading point is always on the yield surface, and eqn (2) we obtain

$$dk = \frac{3/2(\mathbf{r}:d\mathbf{s})}{k + \sqrt{(3/2)(\mathbf{r}:\boldsymbol{\beta})}}. \tag{3}$$

The associated flow rule and the requirement that the uniaxial cyclic behavior is recovered give

$$d\boldsymbol{\varepsilon}^p = \frac{9}{4}\left(\frac{1}{E_t} - \frac{1}{E}\right)_k \cdot \left(\frac{\mathbf{r}:d\boldsymbol{\sigma}}{k^2}\right) \cdot \mathbf{r}.$$

Here E is Young's modulus and $(E_t)_k$ is the tangent modulus measured at flow stress level k. These moduli are obtained from a *stabilized* universal cyclic stress–strain curve, similar to the universal stress–strain curve concept employed in classical plasticity theory. Note that it is how $(E_t)_k$ is determined that distinguishes the current model from the generalization proposed in Ref. [7].

By combining the elastic and plastic parts of the strain increment, the incremental stress–strain relationship can be written in component form as

$$d\varepsilon_{ij} = \left\{\frac{1}{2}\frac{1+\nu}{E}(\delta_{ik}\delta_{jl} + \delta_{jk}\delta_{il}) - \frac{\nu}{E}\delta_{ij}\delta_{kl} + \frac{9}{4}\left(\frac{1}{E_t} - \frac{1}{E}\right)_k \frac{r_{ij}r_{kl}}{k^2}\right\} d\sigma_{kl} \tag{4}$$

or

$$d\sigma_{ij} = \frac{E}{1+\nu}\left\{\frac{1}{2}(\delta_{ik}\delta_{jl} + \delta_{jk}\delta_{il}) + \frac{\nu}{1-2\nu}\delta_{ij}\delta_{kl} - \frac{9}{4}\frac{\left(\frac{1}{E_t} - \frac{1}{E}\right)_k}{\frac{1+\nu}{E} + \frac{3}{2}\left(\frac{1}{E_t} - \frac{1}{E}\right)_k}\frac{r_{ij}r_{kl}}{k^2}\right\} d\varepsilon_{kl} \tag{5}$$

where ν is Poisson's ratio and δ_{ij} is the Kronecker delta. This constitutive equation has the same compact general form as that in classical flow theory.

It is appropriate to mention here that earlier researchers who compared other models with the Mróz discrete multiple yield surface concept were usually concerned with the large extra memory space needed to store the positions of all the yield surfaces. The current model, although having an infinite number of yield surfaces, requires simply the position of the largest yield surface encountered in every *continuous loading path* to be recorded. This surface contains sufficient information to determine the influence of the particular continuous loading path on subsequent deformations. In other words, starting from a virgin state, more information than needed in the classical flow theory is added to the memory whenever unloading takes place ($\mathbf{r}:\mathrm{d}\boldsymbol{\sigma} < 0$); this extra memory space can be eliminated whenever the flow stress level associated with it is exceeded by that in a subsequent loading process. Therefore, depending on the complexity of the loading paths, the size of the memory space *need not* be greatly increased from that required by the widely employed flow theory. (The exception is when the loading history involves cycles of diminishing amplitude.)

APPLICATIONS

In this section, results from the application of the current constitutive model to four complex tension–torsion problems are shown. In the figures, subscripts 11 and 12 are used to denote the tensile and torsional components of the stress (strain) tensor, respectively. Plane-stress conditions are assumed in the 3-direction. The stabilized stress–strain curve is approximated by a power-law curve which gives the following tangent modulus at flow stress level k

$$\left(\frac{1}{E_t} - \frac{1}{E}\right)_k = \frac{1}{E}\left[\left(\frac{k}{\sigma_y}\right)^{1/n-1} - 1\right].$$

Here σ_y is the initial yield stress in uniaxial tension and n is the strain hardening exponent. Values of these constants used in the examples are approximately chosen as listed in the figures. Note that the absolute values of σ_y and E are not included here since they do not affect the results. Their ratio, the yield strain, on the other hand, determines the extent of plastic deformation in a prescribed cyclic history.

All four examples are strain-controlled to enable closer comparisons with existing test results. Note that a strain-controlled experiment can be more precisely controlled than a stress-controlled one. The analysis of a strain-controlled process on the other hand is less straightforward than a stress-controlled process because the adopted model is based on rules established in a stress space. That is, the direction of the stress increment has to be determined first from eqn (5).

The first example involves several sharp strain path changes as shown in Fig. 2(a), to simulate the strain history tested in Ref. [10]. The predicted stress history is displayed in Fig. 2(b), which is observed to resemble closely the experimental results shown in Fig. 2(c), reproduced from Ref. [10]. This qualitative agreement seems to support the hardening behavior derived from the concept of a continuous yield surface field, despite the fact that the size and shape of the initial yield surface are assumed to be constant in the current model but were found to vary after plastic deformation in Ref. [10]. The latter difference may become a source of disagreement in future quantitative comparisons, although at least part of the difference can be attributed to the sensitivity of experimental observations to the adopted subsequent yield surface definition.

Experiments in Ref. [10] also include hours of relaxation time which cannot be accounted for by the current time-independent model. However, the good agreement observed here seems to suggest that the time period of stress relaxation used in Ref. [10] (19 h at maximum) does not have a long-term effect on later deformations and thus can be neglected.

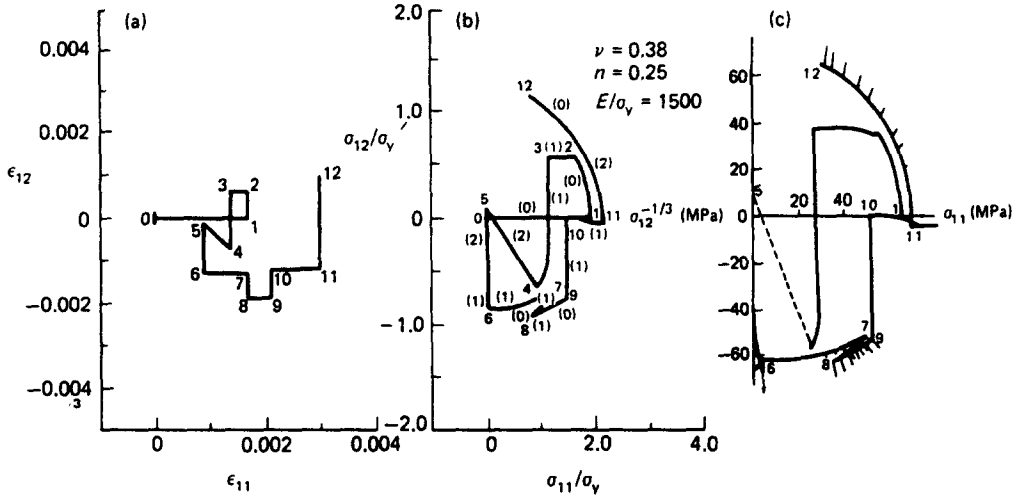

Fig. 2. (a) The prescribed strain path, (b) the predicted stress history and (c) the experimental stress path, from Ref. [10], of a thin aluminum cylindrical tube.

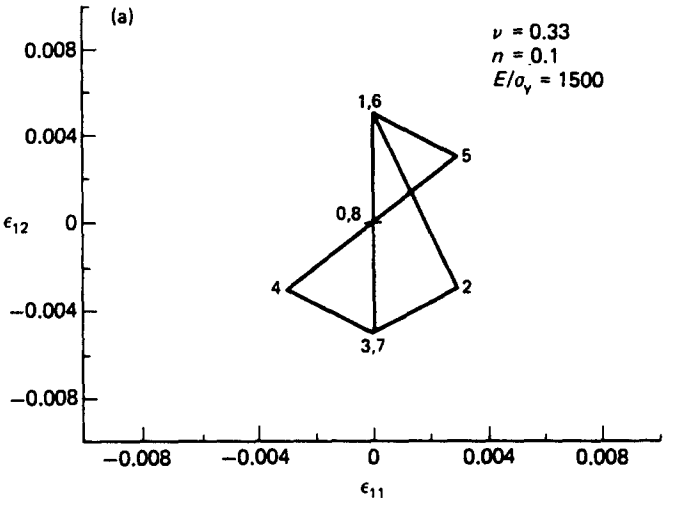

Fig. 3(a). Example 2: the prescribed strain path.

For the next three examples the imposed strain history and three plots of predicted results (for the stress history and the tensile and the torsional stress–strain curves), are presented. They are qualitatively compared with their experimental counterparts from Refs [11–14].

Figure 3(a) shows a strain history containing many different loading modes. This problem was studied in Refs [11, 12]. In Ref. [11] the Mróz multiple yield surface concept incorporated in a two-surface theory was concluded to give better results than the kinematic hardening models with either Prager's or Ziegler's rule. Here the current model predicts similar results as those obtained from the Mróz model in Refs [11, 12]. As shown in Figs 3(b)–(d), these predictions display all the important features observed in experiments (Figs 3(b′)–(d′). The only disagreement, which may be categorized as quantitative, is that the difference in the axial stress level at States 2 and 5 is predicted to be much greater than that measured in experiments.

The last two examples include mode changes as well as load cycles in the strain histories. Cycles of various modes are separated by a reference cycle, denoted by 0 in Figs 4(a) and 5(a). The strain path therefore follows the pattern 0–1–0–2–.... In Figs 4 and 5 the curves representing results from the reference cycles are omitted to give clearer plots. The corresponding experimental results of Fig. 5 are reproduced in Figs 4(b′)–(d′) and

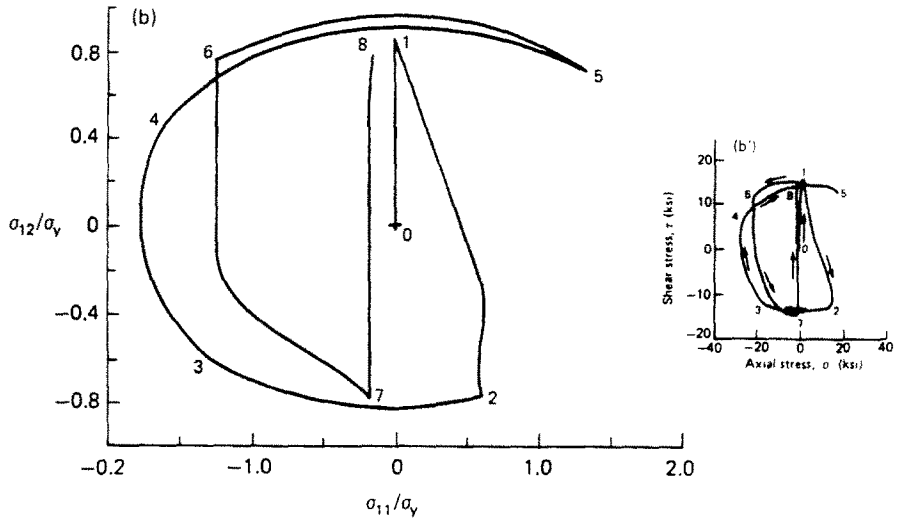

Fig. 3. (b) The predicted stress history and (b') the corresponding experimental result, reproduced from Ref. [11].

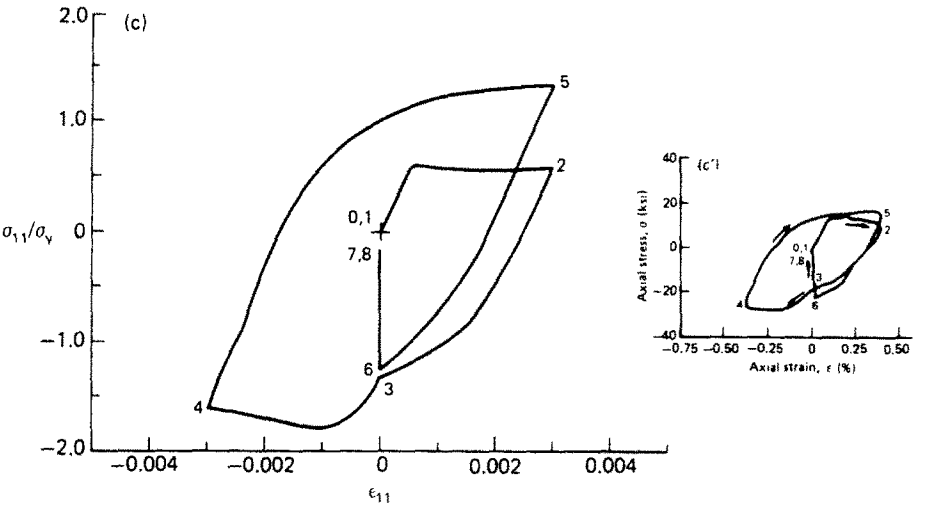

Fig. 3. (c) The predicted tensile stress–strain relationship and (c') the corresponding experimental result from Ref. [11].

5(b')–(d') from Refs [13, 14]. The *qualitative* agreement between the theory and experiments is seen to be remarkably good.

DISCUSSION

In the previous section it is clearly demonstrated that the hardening behavior derived from the generalized Mróz model gives results which are in extremely good qualitative agreement with experimental observations. Here the model is discussed further from various points of view.

Computational aspects

As noted in earlier sections, the assertion that substantially large memory space is needed for Mróz's model is incorrect. By adopting a continuous yield surface field the total additional memory space required depends entirely on the complexity of the history and may not be much more than that required in a classical flow theory calculation. As an example, the number of yield surfaces recorded along each portion of the history is listed in parentheses in Fig. 2(b).

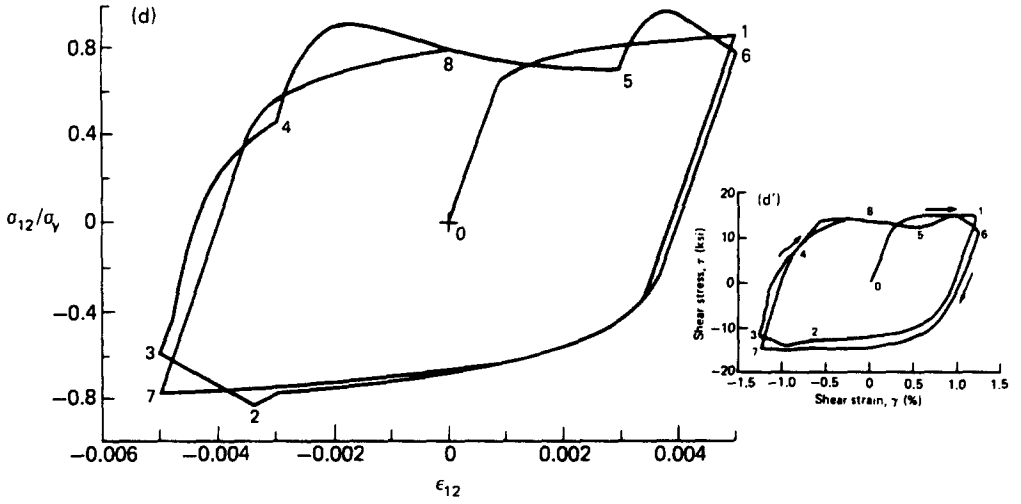

Fig. 3. (d) The predicted torsional stress–strain relationship and (d') the corresponding experimental result from Ref. [11].

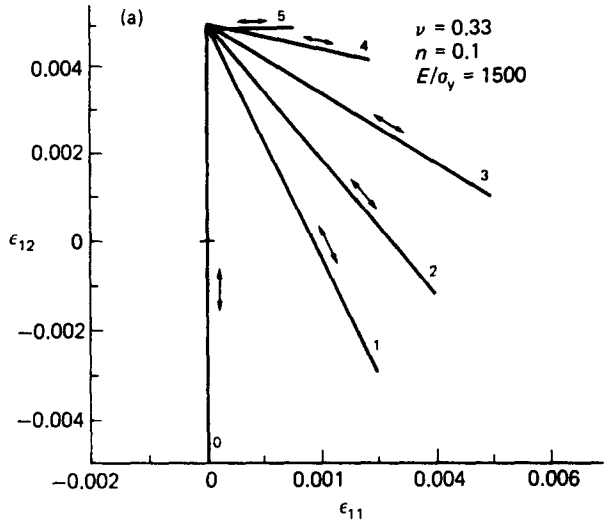

Fig. 4(a). Example 3: the prescribed strain path.

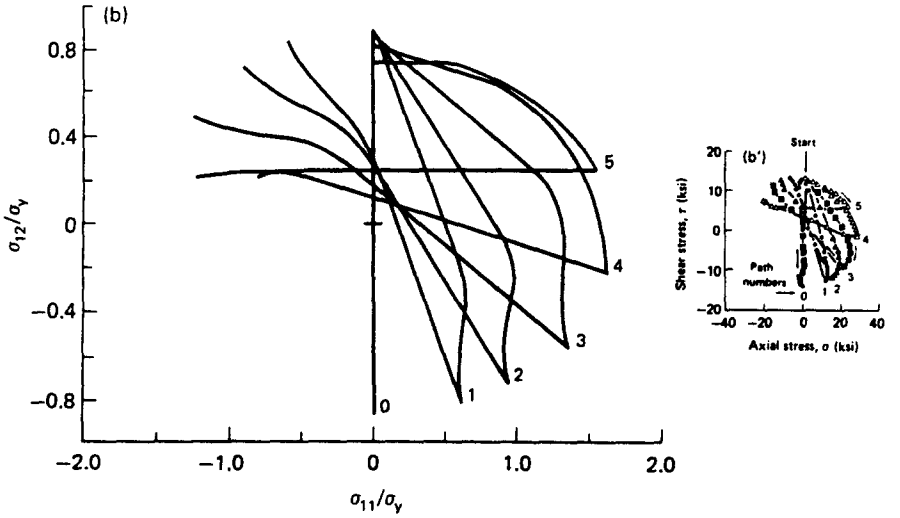

Fig. 4. (b) The predicted stress history and (b') the corresponding experimental result reproduced from Ref. [13].

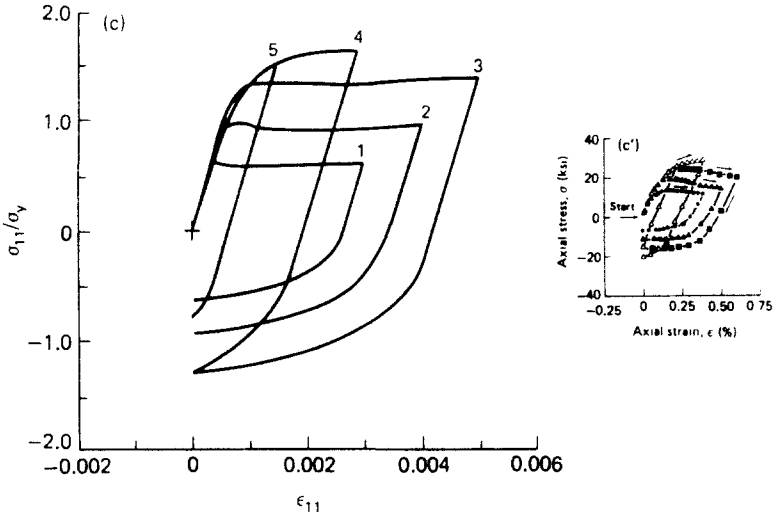

Fig. 4. (c) The predicted tensile stress–strain relationship and (c') the corresponding experimental result from Ref. [13].

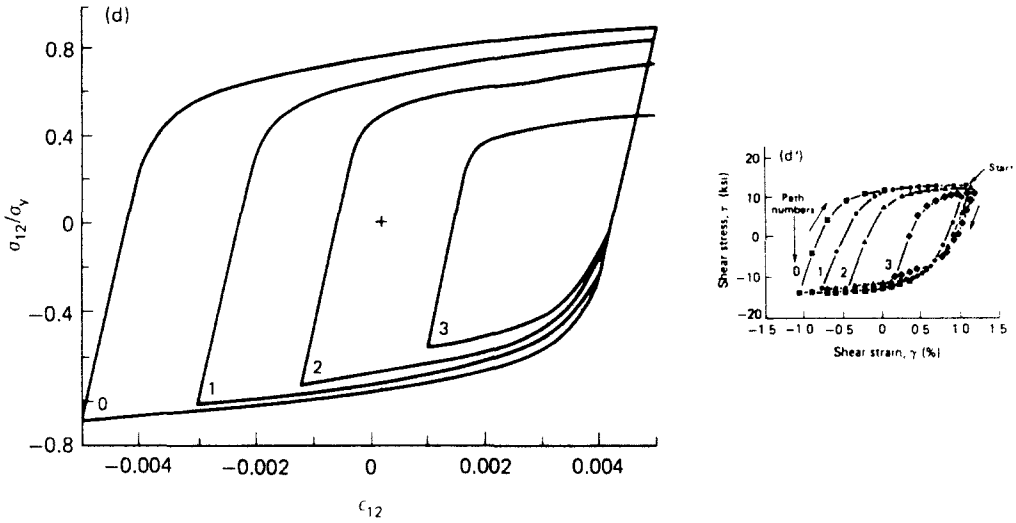

Fig. 4. (d) The predicted torsional stress–strain relationship and (d') the corresponding experimental result from Ref. [13].

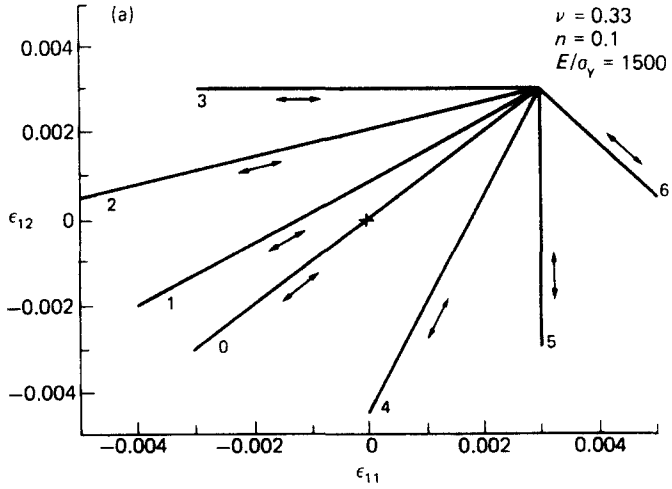

Fig. 5(a). Example 4: the prescribed strain path.

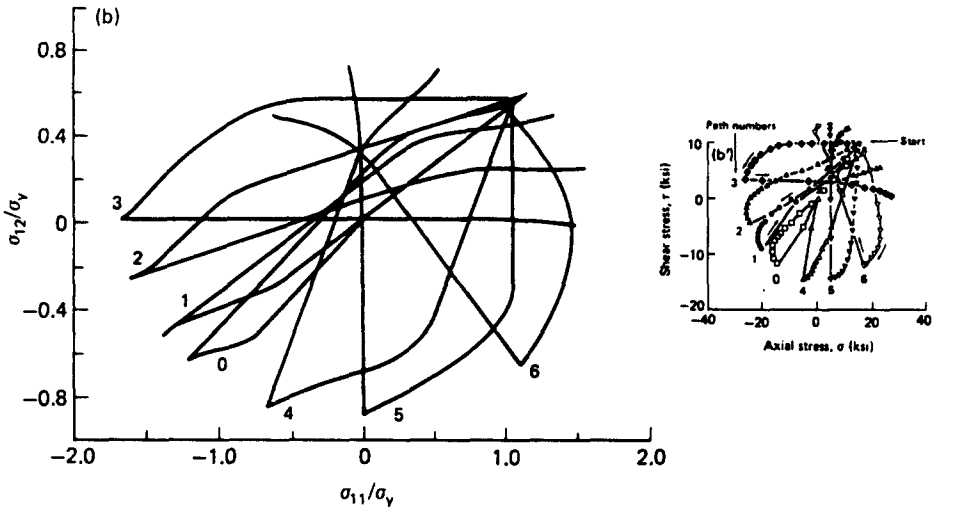

Fig. 5. (b) The predicted stress history and (b') the corresponding experimental result stress history from Ref. [14].

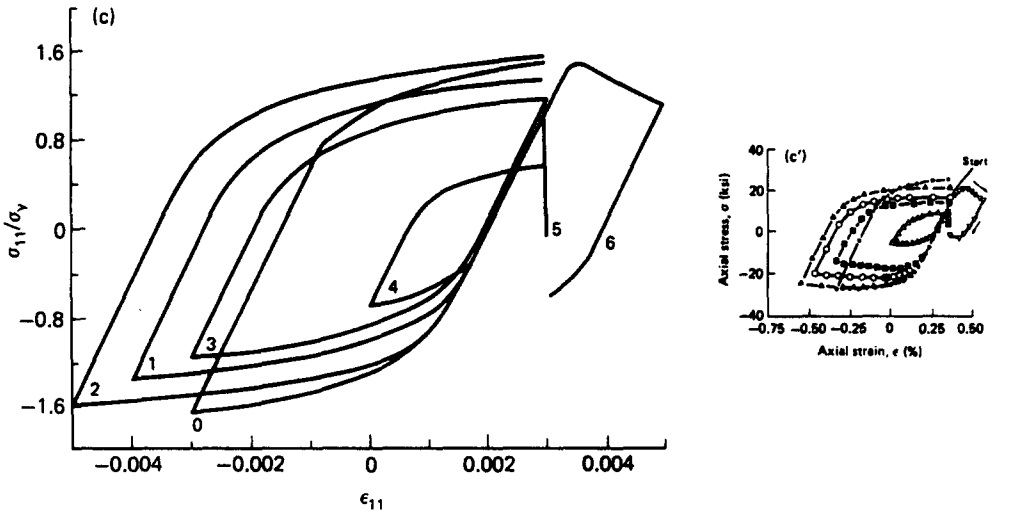

Fig. 5. (c) The predicted tensile stress–strain relationship and (c') the corresponding experimental result from Ref. [14].

Creep and relaxation

The current model, being cyclically stable, does not account for cyclic creep/relaxation phenomena. This deficiency of the current model may be remedied by assuming a transformation rule of the yield surface field that is additionally dependent on mean stress and plastic work.

Softening and hardening

Although the present model contains mechanisms for latent softening and hardening, namely those resulting from earlier loading of different modes, it cannot account for the material structure-related cyclic softening and hardening. Phenomenologically, the latter is likely to be approximated, for instance, by making the size and distribution of the yield surfaces dependent on the amount of plastic work. However, more physical understanding and test data on these types of behavior are desirable to warrant sophisticated manipulations of the yield surface field.

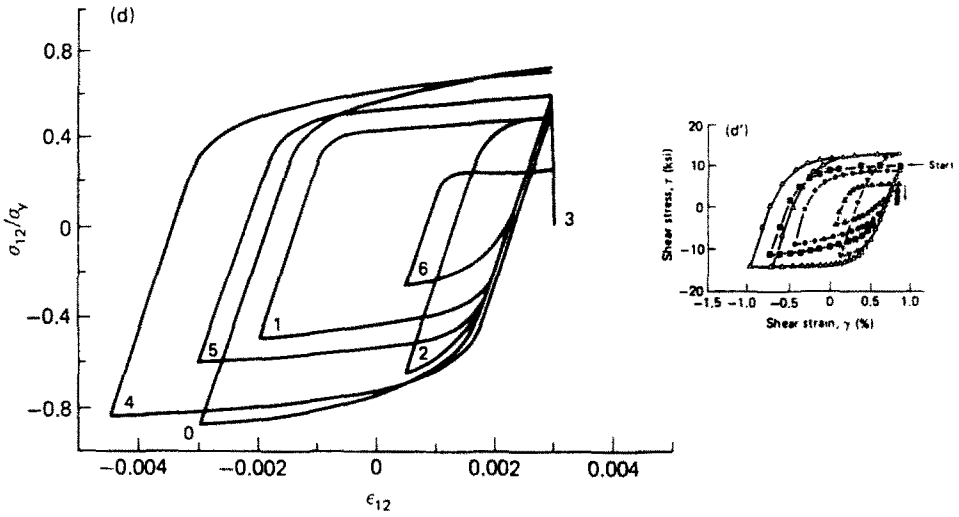

Fig. 5. (d) The predicted torsional stress–strain relationship and (d') the corresponding experimental result from Ref. [14].

Yield function

Here only the von Mises type of yield function is used because of its simple tensor form. The yield function is further assumed to preserve its original form during any elastic–plastic deformation. Such an assumption seems to fail to comply with numerous experimental observations that the shape varies as well as the size of the yield surface. However, it is important to point out that the ability to follow the exact shape variation of the yield surface during plastic deformation should not be over-emphasized, since, except for the subsequent yield stress (upon unloading), the direction of the plastic strain increment, the progression of the plastic stress state and the associated instantaneous modulus are all determined by the *local* behavior of the yield surface near the loading point.

Finally, it is important to realize that the present model only provides a tool to analyze the stress state, strain state and the energy dissipated during complex loading conditions. For the complete design of a structural component, employment of a failure criterion is also important.

Acknowledgement—The author wishes to thank Dr F. A. Conle for helpful discussions.

REFERENCES

1. W. Prager, The theory of plasticity: a survey of recent achievements. *Proc. Instn Mech. Engrs* **169**, 41–50 (1955).
2. H. Ziegler, A modification of Prager's hardening rule. *Q. Appl. Math.* **17**, 55–65 (1959).
3. R. D. Krieg, A practical two surface plasticity theory. *J. Appl. Mech.* **42**, 641–646 (1975).
4. K. C. Valanis, Continuum foundations of endochronic plasticity. *J. Engng Mater. Technol. Trans. ASME* **106**, 367–375 (1984).
5. C.-C. Chu, A three-dimensional model of anisotropic hardening in metals and its application to the analysis of sheet metal formability. *J. Mech. Phys. Solids* **32**, 197–212 (1984).
6. Z. Mróz, On the description of anisotropic work-hardening. *J. Mech. Phys. Solids* **15**, 163–175 (1967).
7. Z. Mróz and V. A. Norris, Elastoplastic and viscoplastic constitutive models, for soils with application to cyclic loading. In *Soil Mechanics—Transient and Cyclic Loads* (Edited by G. N. Pande and O. C. Zienkiewicz), Chap. 8, pp. 173–217. Wiley, New York (1982).
8. Z. Mróz and N. C. Lind, Simplified theories of cyclic plasticity. *Acta Mech.* **22**, 131–152 (1975).
9. Z. Mróz, Hardening and degradation rules for metals under monotonic and cyclic loading. *J. Engng Mater. Technol. Trans. ASME* **105**, 113–118 (1984).
10. A. Phillips and W.-Y. Lu, An experimental investigation of yield surfaces and loading surfaces of pure aluminum with stress-controlled and strain-controlled paths of loading. *J. Engng Mater. Technol. Trans. ASME* **106**, 349–354 (1980).
11. H. S. Lamba and O. M. Sidebottom, Cyclic plasticity for nonproportional paths: Part 2—comparison with predictions of three incremental plasticity models. *J. Engng Mater. Technol. Trans. ASME* **100**, 104–111 (1978).
12. N. T. Tseng and G. C. Lee, Simple plasticity model of two-surface type. *ASCE J. Engng Mech.* **109**, 795–810 (1983).

13. H. S. Lamba and O. M. Sidebottom, Cyclic plasticity for nonproportional paths: Part 1 –cyclic hardening, erasure of memory and subsequent strain hardening experiments. *J. Engng Mater. Technol. Trans. ASME* **100**, 96–103 (1978).
14. H. S. Lamba, Nonproportional cyclic plasticity. T. & A. M. Report No. 413, University of Illinois, Urbana, Illinois.